Applying Sliding Mode Control to a Quadrotor

Toan Le Huu
Faculty of Mechanical Engineering, Vinh Long University of Technology Education, Vinh Long City, Vietnam
toanlh@vlute.edu.vn

Hoang Le Anh
Faculty of Mechanical Engineering, Vinh Long University of Technology Education, Vinh Long City, Vietnam
anhlh@vlute.edu.vn (corresponding author)

Duc Thuan Tran
Faculty of Mechanical Engineering, Vinh Long University of Technology Education, Vinh Long City, Vietnam
thuandauto@yahoo.com

Received: 4 June 2024 | Revised: 29 June 2024 and 18 July 2024 | Accepted: 19 July 2024

 DOI: https://doi.org/10.48084/etasr.8026

ABSTRACT

The current paper discusses the application of Sliding Mode Control (SMC) to a quadcopter. The controller is designed based on the system's nonlinear model. An adaptive sliding mode controller is developed specifically for the quadcopter's attitude subsystem, aiming to mitigate the undesirable vibration phenomena typically associated with conventional sliding mode controllers while ensuring robust trajectory tracking for the quadcopter's attitude. The stability of the proposed controller was verified using the Lyapunov stability theorem. The quadcopter Unmanned Aerial Vehicle (UAV) model and the performance of the proposed controller were simulated and validated in MATLAB/SIMULINK environment. The results demonstrate that the proposed controller effectively positions the quadcopter with minimal error, maintaining the UAVs flight along the prescribed trajectory. Additionally, it performs well in trajectory tracking under collision noise and vibration reduction conditions.

Keywords-sliding mode control; flight trajectory; UAV; quadrotor

I. INTRODUCTION

The use of Unmanned Aerial Vehicles (UAVs), especially quadrotors, has become popular in military, academic research, and commerce. UAVs are utilized in 3D indoor reconstruction from photogrammetry [1, 2]. A quadrotor has many advantages, such as vertical takeoff and landing, hovering ability, small size, high mobility, and low price. Choosing the right controller for a quadrotor UAV remains challenging for both indoor and outdoor fields. This occurs because the driving characteristics of the quadrotor are a combination of translational and rotational dynamics as well as high nonlinearity. Many control techniques for quadrotor systems have been proposed in the literature. Authors in [3-7] used a PID controller to stabilize yaw angle and yaw angle motion. However, when employing a PID controller, it cannot meet the requirements in noisy conditions. Other attempts to control the quadcopter were made based on feedback linearization [8-11]. This technique is limited for some applications due to its lack of precision. In [12-15], the authors solved the problem of system stability in the presence of environmental disturbances. However, the FL controller is not really suitable for sensor noise. Therefore, this study deployed a sliding mode controller to stabilize the quadrotor flight trajectory in the presence of environmental disturbances. The article applies the control of a quadrotor system based on Sliding Mode Control (SMC).

II. RESEARCH CONTENT

A. Dynamic Model of the Quadrotor

The quadrotor system dynamics modeling of [16] was used. The mathematical model is written as a state space equation:

$$\dot{\mathrm{X}} = f\left(\mathrm{X}, U\right)$$

where X is the state vector, U is the control input vector, and $\mathrm{X} = \left[\Phi, \dot{\Phi}, \theta, \dot{\theta}, \Psi, \dot{\Psi}, x, \dot{x}, y, \dot{y}, z, \dot{z}\right]^T \in \Re^{12}$. The state space vector can be rewritten as:

$$\mathrm{X} = \left[x_1, x_2, x_3, x_4, x_5, x_6, x_7, x_8, x_9, x_{10}, x_{11}, x_{12}\right]^T \in \Re^{12}$$

$$U = \left[U_1 U_2 U_3 U_4\right]^T$$

$$\begin{cases} \ddot{\Phi} = \dfrac{U_2}{I_x} - \dfrac{c_{d\Phi}\dot{\Phi}^2}{I_x} - \dfrac{I_r\Omega_r\dot{\theta}}{I_x} - \dfrac{\left(I_z - I_y\right)\dot{\theta}\dot{\psi}}{I_x} \\ \ddot{\theta} = \dfrac{U_3}{I_y} - \dfrac{c_{d\theta}\dot{\theta}^2}{I_y} + \dfrac{I_r\Omega_r\dot{\Phi}}{I_y} - \dfrac{\left(I_x - I_z\right)\dot{\Phi}\dot{\psi}}{I_y} \\ \ddot{\psi} = \dfrac{U_4}{I_z} - \dfrac{c_{d\Psi}\dot{\Psi}^2}{I_z} - \dfrac{\left(I_y - I_x\right)\dot{\theta}\dot{\Phi}}{I_z} \\ \ddot{x} = \dfrac{U_1\left(\mathrm{c}\psi s\theta c\Phi + s\Psi s\Phi\right)}{m} - \dfrac{c_{dx}\dot{x}}{m} \\ \ddot{y} = \dfrac{U_1\left(c\Phi s\theta s\psi - s\Phi c\psi\right)}{m} - \dfrac{c_{dy}\dot{y}}{m} \\ \ddot{z} = \dfrac{U_1 c\Phi c\theta}{m} - \dfrac{c_{dz}\dot{z}}{m} - g \end{cases} \quad (1)$$

where U_1, U_2, U_3, U_4 are the height, roll (φ), pitch (θ), yaw angle (Ψ) controllers, respectively. I_z, I_y, and I_x denote the moment of inertia at the z -, y -, and x - axes of the quadrotor, respectively, I_r is the z - axis moment of inertia of the rotor and Ω_r is its total angular velocity. c and s denote the cosine and s sine functions. C_{dxyz} is the drag coefficient in x, y, z directions and $C_{d\Phi\theta\Psi}$ is the aerodynamic friction coefficient. The sliding mode controller works based on intermediate control laws for a series of state variables defined as follows:

$$\lambda_1 = \frac{I_y - I_z}{I_x}; \lambda_2 = -\frac{c_{d\Phi}}{I_x}; \lambda_3 = -\frac{J_r}{I_x}; \lambda_4 = \frac{I_z - I_x}{I_y}; \lambda_5 = -\frac{c_{d\theta}}{I_y};$$

$$\lambda_6 = \frac{J_r}{I_y}; \lambda_7 = \frac{I_x - I_y}{I_z}; \lambda_8 = -\frac{c_{d\Psi}}{I_z}; \lambda_9 = -\frac{c_{dx}}{m}; \lambda_{10} = -\frac{c_{dy}}{m};$$

$$\lambda_{11} = -\frac{c_{dz}}{m}; a_1 = \frac{1}{I_x}; a_2 = \frac{1}{I_y}; a_3 = \frac{1}{I_z}$$

$$U_x = \left(c_{\phi d}s_{\theta d}c_{\psi} - s_{\phi d}s_{\psi}\right) = c_{x_1}s_{x_3}c_{x_5} - s_{x_1}s_{x_5}$$

$$U_y = \left(c_{\phi d}s_{\theta d}s_{\psi} - s_{\phi d}c_{\psi}\right) = c_{x_1}s_{x_3}s_{x_5} - s_{x_1}c_{x_5}$$

Equation (1) can be rewritten as:

$$\begin{bmatrix} \dot{x}_1 \\ \dot{x}_2 \\ \dot{x}_3 \\ \dot{x}_4 \\ \dot{x}_5 \\ \dot{x}_6 \\ \dot{x}_7 \\ \dot{x}_8 \\ \dot{x}_9 \\ \dot{x}_{10} \\ \dot{x}_{11} \\ \dot{x}_{12} \end{bmatrix} = \begin{bmatrix} x_2 \\ \lambda_1 x_4 x_6 + a_1 U_2 + \lambda_2 x_2^2 + \lambda_3 \Omega_r x_4 \\ x_4 \\ \lambda_4 x_2 x_6 + a_2 U_3 + \lambda_5 x_4^2 + \lambda_6 \Omega_r x_2 \\ x_6 \\ \lambda_7 x_2 x_4 + a_3 U_4 + \lambda_8 x_6^2 \\ x_8 \\ U_X U_1 / m + \lambda_9 x_8 \\ x_{10} \\ U_y U_1 / m + \lambda_{10} x_{10} \\ x_{12} \\ -g + \left(\mathrm{c}\Phi\,\mathrm{c}\,\theta\right) U_1 / m + \lambda_{11} x_{12} \end{bmatrix} \quad (2)$$

B. Controller Design

1) Selection of the Sliding Surface

The task of designing the control law of the sliding function is to ensure that all state trajectories of the system gradually approach the sliding surface and maintain that state right after the sliding surface is captured. The desired equation has the form of (3):

$$\mathrm{B}(x) = \left(\mathrm{N}_x + \frac{d}{dt}\right)^{f-1} \quad (3)$$

where x is the control variable or state vector and $e\left(x\right)$ is the tracking error defined as $x_d - x$. N_x is a positive constant that interprets the surface dynamics and f is the relative order of the sliding mode controller.

$$\mathrm{B}(x) = \mathrm{N}_x e(x) + \dot{e}(x) \quad (4)$$

This approach is based on the Lyapunov function to access the conditions of the sliding surface [17]. The Lyapunov function is described as:

$$\mathrm{T} = \frac{1}{2}\mathrm{B}^2 \quad (5)$$

to stabilize $\dot{\mathrm{T}} < 0$ it means that: $\dot{\mathrm{T}} = \mathrm{B}\dot{\mathrm{B}} < 0$.

The purpose of the proposed controller is to achieve asymptotic position and attitude tracking for the quadrotor achieved using an SMC strategy. This is accomplished by reducing the tracking error to zero to attain the required tracking performance. The first stage of the SMC method involves guiding the system states towards a predetermined sliding surface and a stability control law is formulated to ensure that the system stays on that surface.

$$e_i = x_{id} - x_i, e_{i+1} = \dot{e}_1 \quad (6)$$

where i = 1,2…..,6.

$$\dot{\mathrm{B}}_i = -L_i \mathrm{Sign}\left(\mathrm{B}_i\right) \quad (7)$$

where $\mathrm{L_i} > 0$ indicates constant speed.

$$\mathrm{Sign}\left(\mathrm{B}_i\right) = \begin{cases} 1, & \mathrm{B}_i > 0 \\ 0, & \mathrm{B}_i = 0 \\ -1, & \mathrm{B}_i < 0 \end{cases} \quad (8)$$

The glide mode is based on the approach law including phase approach and glide phase. The drive system approaches phase to maintain system stability. The sliding phase ensures sliding to a balanced position. This law limits the switching parameters B to a constant speed L_i. If the value of the L_i is too small, the time to reach it will be long. A too large value will cause chattering, so choosing the right value determines the success of the controller. The sliding surface of the sliding mode controller is selected from (6). From there, the sliding surface can be selected based on the tracking error as follows:

Tracking error and sliding surface for roll, pitch, and yaw dynamics are provided by (9), (10), and (11), respectively:

$$\phi_{\mathrm{e}} = \Phi_{\mathrm{d}} - \Phi = \mathrm{e}_1, \mathrm{B}_1 = \mathrm{N}_1\Phi_{\mathrm{e}} + \dot{\Phi}_{\mathrm{e}} \quad (9)$$

$$\theta_{\mathrm{e}} = \theta_{\mathrm{d}} - \theta = \mathrm{e}_2, \mathrm{B}_2 = \mathrm{N}_2\theta_{\mathrm{e}} + \dot{\theta}_{\mathrm{e}} \quad (10)$$

$$\psi_e = \psi_d - \psi = e_3, \mathrm{B}_3 = \mathrm{N}_3\psi_e + \psi_e \quad (11)$$

The vertical surface along the X and Y directions is given by:

$$x_{\mathrm{d}} - x = \mathrm{e}_4 = x_{\mathrm{e}}, \mathrm{B}_4 = \mathrm{N}_4 x_{\mathrm{e}} + \dot{x}_{\mathrm{e}} \quad (12)$$

$$y_{\mathrm{d}} - y = \mathrm{e}_5 = y_{\mathrm{e}}, \mathrm{B}_5 = \mathrm{N}_5 y_{\mathrm{e}} + \dot{y}_{\mathrm{e}} \quad (13)$$

Tracking error and sliding surface error for the altitude dynamics are provided by:

$$\mathrm{B}_6 = \mathrm{N}_6 \mathrm{z}_{\mathrm{e}} + \dot{z}_{\mathrm{e}},\ \mathrm{z}_{\mathrm{e}} = \mathrm{z}_{\mathrm{d}} - \mathrm{z} = \mathrm{e}_6 \quad (14)$$

In the above equations N_1, ……., N_6 satisfy the Hurwitz condition and are greater than 0.

The position controller is designed to control the UAV translational dynamics model in the X and Y directions. Consider U_x and U_y are the directions of U_1 . Directional control is used to direct the ψ movement (left and right movement).

The attitude controller is designed to stabilize the yaw, pitch, and roll angles of the quadrotor.

The altitude controller is designed to stabilize the altitude or vertical movement along the *z*-axis.

The control law is designed based on the sliding surface of the position, altitude, attitude, and direction of the quadrotor.

2) Roll and Pitch Angles SMC Design

The tracking error and the transition surface for the roll angle are defined in (9) and the derivative of the sliding surface is:

$$\begin{aligned} &\dot{\mathrm{B}}_1 = \mathrm{N}_1\dot{e}_1 + \dot{e}_1 = \mathrm{N}_1\left(\dot{\Phi}_{\mathrm{d}} - \dot{\Phi}\right) + \ddot{\Phi}_{\mathrm{d}} - \ddot{\Phi}; \\ &\mathrm{B}_1 = -L_1\mathrm{Sign}\left(\mathrm{B}_1\right); \end{aligned} \quad (15)$$

From (2) we get:

$$\ddot{\Phi} = \dot{x}_2 = \lambda_1 x_4 x_6 - \lambda_2 x_2^2 - \lambda_3\Omega_r x_4 + a_1 U_2$$

which is substituted into (15) and U_2 is calculated by:

$$U_2 = \frac{1}{a_1}\begin{bmatrix} \mathrm{x}_{1d} - \lambda_1 \mathrm{x}_4 \mathrm{x}_6 - \lambda_2 \mathrm{x}_2^2 - \lambda_3\Omega_1 \mathrm{x}_4 + \mathrm{N}_1\dot{e}_1 \\ +L_1\mathrm{Sign}\left(\mathrm{B}_1\right) \end{bmatrix} \quad (16)$$

For the sliding surface dynamics and pitch angle tracking error determined in (10), the derivative of the sliding surface is given by:

$$\dot{\mathrm{B}}_2 = \mathrm{N}_2\dot{e}_2 + \ddot{e}_2 = \mathrm{N}_2\dot{\theta}_e + \ddot{\theta}_e = \mathrm{N}_2\left(\dot{\theta}_d - \dot{\theta}\right) + \ddot{\theta}_d - \ddot{\theta} \quad (17)$$

Substituting $\dot{\mathrm{B}}_2$ from (7) and $\ddot{\theta}$ from (2) into (17) allows us to calculate U_3:

$$U_3 = \frac{1}{a_2}\begin{bmatrix} \dot{x}_{3d} - \lambda_4 x_2 x_6 - \lambda_5 x_4^2 - \lambda_6\Omega_r x_2 + \mathrm{N}_2\dot{e}_2 \\ +\mathrm{L}_2\mathrm{Sign}\left(\mathrm{B}_2\right) \end{bmatrix} \quad (18)$$

3) SMC Design for Direction and Yaw

The error and sliding surface of the quadrotor are determined by (11). The derivative of the sliding surface is given by:

$$\begin{aligned} \dot{\mathrm{B}}_3 &= \mathrm{N}_3\dot{e}_3 + \ddot{e}_3 = \mathrm{N}_3\psi_e + \ddot{\psi}_e \\ &= \mathrm{N}_3\left(\dot{\psi}_{\mathrm{d}} - \dot{\psi}\right) + \ddot{\psi}_{\mathrm{d}} - \ddot{\psi} \end{aligned} \quad (19)$$

Replacing (7) and (2) in (19) gives:

$$U_4 = \frac{1}{a_3}\begin{bmatrix} \dot{x}_{5d} - \lambda_7 x_2 x_4 - \lambda_8 x_6^2 + \mathrm{N}_3\dot{e}_3 \\ +L_3\mathrm{Sign}\left(\mathrm{B}_3\right) \end{bmatrix} \quad (20)$$

4) SMC Design for Z-axis Translational Motion

The relationship between the control input U_1 and the gravitational and aerodynamic forces along the z-axis is used to determine U_1. The sliding surface and the error of the *z*- axis dynamics are determined in (14). The derivative is given by:

$$\begin{aligned} &\mathrm{B}_6 = \mathrm{N}_6\dot{\mathrm{e}}_6 + \ddot{\mathrm{e}}_6 = \mathrm{N}_6\dot{z}_e + \ddot{z}_e = \mathrm{N}_6\left(\dot{z}_d - \dot{z}\right) + \ddot{z}_d - \ddot{z}; \\ &\dot{\mathrm{B}}_6 = -L_6\mathrm{Sign}\left(\mathrm{B}_6\right); \end{aligned} \quad (21)$$

Substituting the translational dynamic equation Z in (2) into (21), the height control input U_1 is calculated by:

$$\mathrm{U}_1 = \frac{\mathrm{m}}{c_{x1}c_{x3}}\begin{bmatrix} \ddot{z}_{\mathrm{d}} - \lambda_{11}\mathrm{x}_{12} + \mathrm{g} + \mathrm{N}_6\dot{\mathrm{e}}_6 \\ +L_6\mathrm{Sign}\left(\mathrm{B}_6\right) \end{bmatrix} \quad (22)$$

5) SMC Design of X and Y Axes Translation Motion

The same method is followed to formulate the control laws U_x and U_y to stabilize the corresponding positions of the quadcopter in the X and Y directions. The dynamic force in the X direction of the selected sliding surface and the error are described in (12) and the derivative is calculated as follows:

$$\begin{aligned} &\dot{\mathrm{B}}_4 = \mathrm{N}_4\dot{\mathrm{e}}_4 + \ddot{e}_4 = \mathrm{N}_4\dot{x}_{\mathrm{e}} + \ddot{x}_{\mathrm{e}} = \mathrm{N}_4\left(\dot{x}_{\mathrm{d}} - \dot{x}\right) + \ddot{x}_{\mathrm{d}} - \ddot{x}; \\ &\dot{\mathrm{B}}_4 = -L_4\mathrm{Sign}\left(\mathrm{B}_4\right); \end{aligned} \quad (23)$$

Substituting the dynamic equation in the X direction in (2) into (23), the desired position controller in the X direction U_x is obtained as:

$$\mathrm{U}_{\mathrm{x}} = \frac{\mathrm{m}}{\mathrm{U}_1}\begin{bmatrix} \ddot{x}_{7\,\mathrm{d}} - \lambda_9 \mathrm{x}_8 + \mathrm{N}_4\ddot{e}_4 \\ +L_4\mathrm{Sign}\left(\mathrm{B}_4\right) \end{bmatrix} \quad (24)$$

For position dynamics in the Y direction, the selected sliding surface and error are described in (13) and the derivative is given by:

$$\begin{aligned}\dot{B}_5 &= N_5\dot{e}_5 + \ddot{e}_5 = N_5\dot{y}_e + \ddot{y}_e \\ &= N_5\left(\dot{y}_d - \dot{y}\right) + \ddot{y}_d - \ddot{y} \\ \dot{B}_5 &= -L_5 \mathrm{Sign}\left(B_5\right)\end{aligned} \quad (25)$$

Substituting the dynamic equation in the Y direction in (2) into (25), the desired position controller in the Y direction U_y is obtained as:

$$U_y = \frac{m}{U_1}\begin{bmatrix}\ddot{x}_{9d} - \lambda_{10}x_{10} + N_5\dot{e}_5 \\ +L_5 \mathrm{Sign}\left(B_5\right)\end{bmatrix} \quad (26)$$

C. Chattering Reduction

The slide controller may vibrate due to the function Sign(B_i). The control law in (16), (18), (20), (22), (24), (26) in a finite time controls the direction and position of the quadrotor and will converge to the reference position. However, the function Sign(B_i) will cause vibration due to chattering around the sliding surface. Some studies attempted to reduce the vibration caused by chattering by trying different methods such as neural networks and boundary conditions around the SMC sliding surface [18, 19]. In this study, creating a boundary layer around the sliding surface is used to reduce the vibration of the system. To limit the effects of vibrations, the saturation function Sat(B_i) is used instead of the Sign(B_i) function. The saturation function equation is [20]:

$$\mathrm{Sat}(B(i)) = \begin{cases}1, & B(i) > \Delta \\ \dfrac{B(i)}{\Delta}, & B(i) \le \Delta \\ -1, & B(i) < -\Delta\end{cases} \quad (27)$$

where Δ is the boundary layer. The essence of the saturation function is to select the switch control at the boundary layer and apply normal feedback conditions. In this way, the chattering phenomenon is completely limited.

The SMC controller relies on the saturation function. The limit on the quadrotor system is rewritten as follows:

$$\begin{aligned}U_2 &= \frac{1}{a_1}\begin{bmatrix}x_{1d} - \lambda_1 x_4 x_6 - \lambda_2 x_2^2 - \lambda_3 \Omega_1 x_4 + N_1\dot{e}_1 \\ +L_1 \mathrm{Sat}\left(B_1\right)\end{bmatrix} \\ U_3 &= \frac{1}{a_2}\begin{bmatrix}\dot{x}_{3d} - \lambda_4 x_2 x_6 - \lambda_5 x_4^2 - \lambda_6 \Omega_r x_2 + N_2\dot{e}_2 \\ +L_2 Sat\left(B_2\right)\end{bmatrix} \\ U_4 &= \frac{1}{a_3}\begin{bmatrix}\dot{x}_{5d} - \lambda_7 x_2 x_4 - \lambda_8 x_6^2 + N_3\dot{e}_3 \\ +L_3 \mathrm{Sat}\left(B_3\right)\end{bmatrix} \\ U_x &= \frac{m}{U_1}\left[\ddot{x}_{7\,d} - \lambda_9 x_8 + N_4\ddot{e}_4 + L_4 \mathrm{Sat}\left(B_4\right)\right] \\ U_y &= \frac{m}{U_1}\left[\ddot{x}_{9d} - \lambda_{10} x_{10} + N_5\dot{e}_5 + L_5 \mathrm{Sat}\left(B_5\right)\right] \\ U_1 &= \frac{m}{c_{x1}c_{x3}}\left[\ddot{z}_d - \lambda_{11} x_{12} + g + N_6\dot{e}_6 + L_6 \mathrm{Sat}\left(B_6\right)\right]\end{aligned} \quad (28)$$

When using control law (28), the actual position of the quadrotor will ensure convergence to the reference position in finite time and significantly limit the chattering phenomenon around the sliding surface.

III. RESULTS AND DISCUSSION

A. Simulated Results without Noise

The control goal is to track the trajectory. Figure 1 shows the SIMULINK model of a quadcopter with position and attitude control modules in the loop. The system was tested with and without interference. The UAV simulation parameters are displayed in Table I. Simulations were conducted to evaluate the performance of the sliding mode controller using the sat and sign functions. Figures 2, 3, 4 show 3D and 2D orbits, position, and attachment angles.

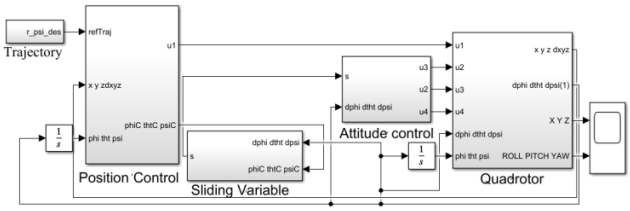

Fig. 1. Simulink model of the SMC system.

TABLE I. UAV PARAMETERS USED IN SIMULATIONS

Parameter	Value	Unit
K_f	13328×10^{-4}	Kg.m
K_M	13858×10^{-5}	Kg.m^2
m	1.4	Kg
l	0.56	m
I_x	0.05	Kg.m^2
I_y	0.05	Kg.m^2
I_z	0.24	Kg.m^2
g	9.81	m.s^2

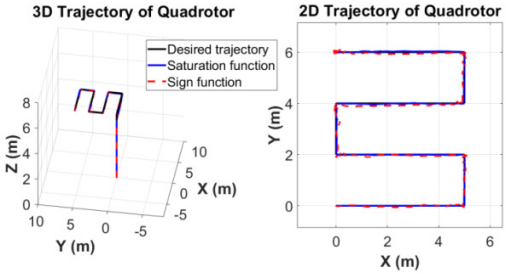

Fig. 2. Quadrotor's 3D and 2D orbits.

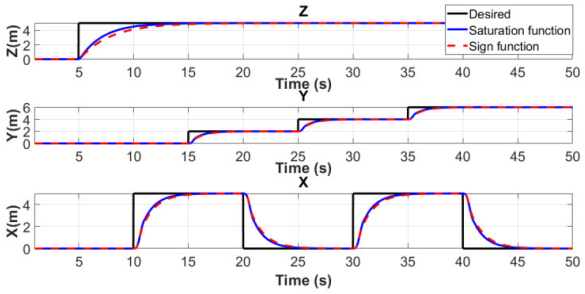

Fig. 3. Tracking the Z, Y, X positions of the quadrotor.

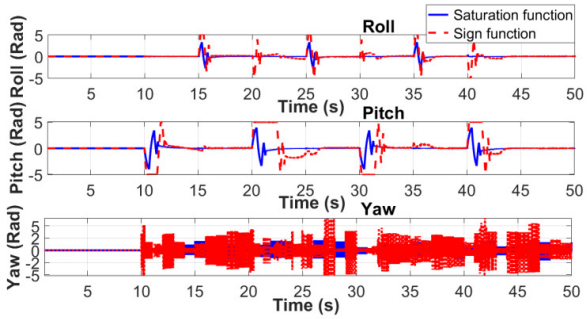

Fig. 4. Quadrotor attachment angles with saturation function and sign function.

In Figures 2 and 3, it can be observed that the position tracking error of the controller is very good with the error being less than 0.1 m. However, the response time of the controller when using the sign function is 0.2 - 0.5 s larger than that acquired when using the saturation function (see Figure 4). The quadrotor's attachment angle when utilizing the saturation function will reduce oscillations caused by chattering phenomenon more than the sign function. The UAV trajectory Root Mean Square (RMS) tracking error without noise with the SMC set when using the saturation function is 0.5 m, while the RMS with the sign function is 0.9 m.

B. Simulated Results witht Noise

White noise (sensor noise) signal was added to the simulations with the proposed controller with $P = 0.0002$ w and $T = 0.001$ s, as shown in Figure 5. Noise was applied as an input at time $t = 10$ s. Figures 6, 7, 8 exhibit the quadrotor's tracking orbits in 3D, 2D, Z, Y.

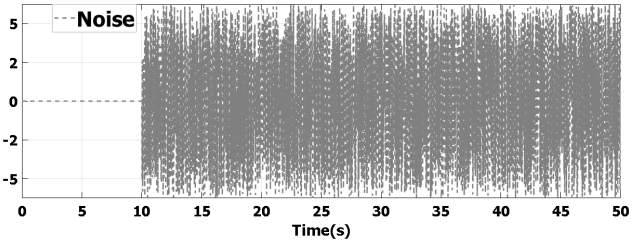

Fig. 5. White noise impact from the 10th second.

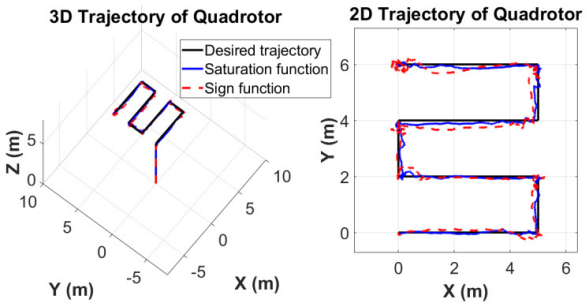

Fig. 6. Quadrotor's 3D and 2D trajectory (there is noise from $t = 10$ s).

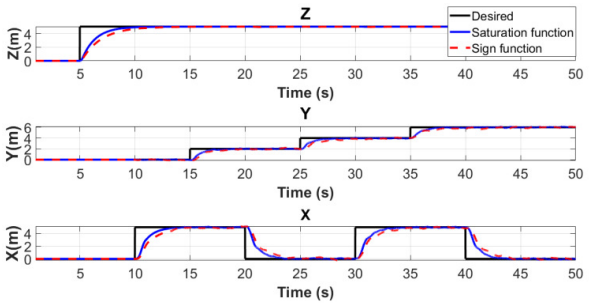

Fig. 7. Tracking positions Z, Y, X (there is noise from $t = 10$ s).

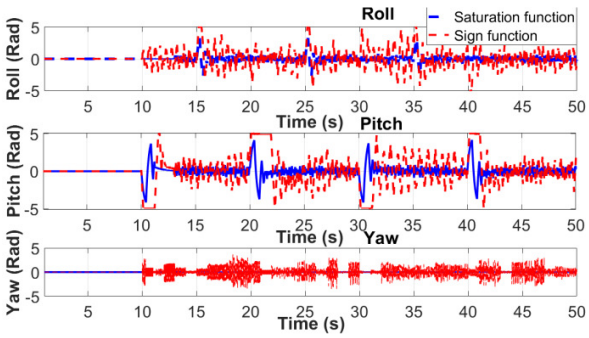

Fig. 8. Quadrotor attachment angles with saturation function and sign functions (there is noise from $t = 10$ s).

It can be concluded that the controller is robust enough to withstand the influence of disturbances. The system becomes unstable when there is additional noise. Figures 6 and 7 demonstrate that is takes about 5 s for all coordinates to converge to the desired value. In Figure 8, when using the sign function in an environment with additional noise, the tracking angles will jerk with large amplitudes due to the chattering phenomenon. When utilizing the sat function, it can be seen that the amplitude is stable, which helps the system to track location better. The UAV trajectory tracking RMS error when there is noise when using the saturation function is 2.47 m, while the RMS with the sign function is 3.09 m.

IV. CONCLUSION

The proposed sliding mode controller has demonstrated stability with the ability to move and track the trajectory of the UAV. A non-linear model and a sliding mode-based controller have been synthesized to ensure noise reduction, which can improve the stability under the influence of disturbances. In addition, in a noise-free environment, the proposed controller with the saturation function has a negligible RMS error in comparison to the 0.9 m error acquired with the sign function. In a noisy environment, the RMS error will be greatly affected, being 2.47 when using the saturation function and 3.09 when using the sign function. However, the proposed control law has helped the UAV operate stably at the reference altitude and track the trajectory in the simulation. The next development direction can apply the SMC controller with the saturation function in real conditions with natural disturbances.

REFERENCES

[1] A. N. Sazaly, M. F. M. Ariff, and A. F. Razali, "3D Indoor Crime Scene Reconstruction from Micro UAV Photogrammetry Technique,"

Engineering, Technology & Applied Science Research, vol. 13, no. 6, pp. 12020–12025, Dec. 2023, https://doi.org/10.48084/etasr.6260.

[2] S. Saeedi, C. Thibault, M. Trentini, and H. Li, "3D Mapping for Autonomous Quadrotor Aircraft," *Unmanned Systems*, vol. 5, no. 3, pp. 181–196, Jul. 2017, https://doi.org/10.1142/S2301385017400064.

[3] T. Susanto, M. Bayu Setiawan, A. Jayadi, F. Rossi, A. Hamdhi, and J. Persada Sembiring, "Application of Unmanned Aircraft PID Control System for Roll, Pitch and Yaw Stability on Fixed Wings," in *International Conference on Computer Science, Information Technology, and Electrical Engineering*, Banyuwangi, Indonesia, Oct. 2021, pp. 186–190, https://doi.org/10.1109/ICOMITEE53461.2021. 9650314.

[4] Q. Li, G. Shi, J. Wei, and Y. Lin, "Yaw Stability Control of Active Front Steering with Fractional-Order PID Controller," in *International Conference on Information Engineering and Computer Science*, Wuhan, China, Dec. 2009, pp. 1–4, https://doi.org/10.1109/ICIECS.2009. 5366433.

[5] A. L. Salih, M. Moghavvemi, H. A. F. Mohamed, and K. S. Gaeid, "Modelling and PID controller design for a quadrotor unmanned air vehicle," in *International Conference on Automation, Quality and Testing, Robotics*, Cluj-Napoca, Romania, Dec. 2010, vol. 1, pp. 1–5, https://doi.org/10.1109/AQTR.2010.5520914.

[6] Faizan. A. Warsi *et al.*, "Yaw, Pitch and Roll controller design for fixed-wing UAV under uncertainty and perturbed condition," in *10th International Colloquium on Signal Processing and its Applications*, Kuala Lumpur, Malaysia, Mar. 2014, pp. 151–156, https://doi.org/10.1109/CSPA.2014.6805738.

[7] L. Martins, C. Cardeira, and P. Oliveira, "Inner-outer feedback linearization for quadrotor control: two-step design and validation," *Nonlinear Dynamics*, vol. 110, no. 1, pp. 479–495, Sep. 2022, https://doi.org/10.1007/s11071-022-07632-y.

[8] L. Martins, C. Cardeira, and P. Oliveira, "Feedback Linearization with Zero Dynamics Stabilization for Quadrotor Control," *Journal of Intelligent & Robotic Systems*, vol. 101, no. 1, Dec. 2020, Art. no. 7, https://doi.org/10.1007/s10846-020-01265-2.

[9] E. Kuantama, I. Tarca, and R. Tarca, "Feedback Linearization LQR Control for Quadcopter Position Tracking," in *5th International Conference on Control, Decision and Information Technologies*, Thessaloniki, Greece, Apr. 2018, pp. 204–209, https://doi.org/10.1109/CoDIT.2018.8394911.

[10] Z. Cai, S. Zhang, and X. Jing, "Model Predictive Controller for Quadcopter Trajectory Tracking Based on Feedback Linearization," *IEEE Access*, vol. 9, pp. 162909–162918, Jan. 2021, https://doi.org/ 10.1109/ACCESS.2021.3134009.

[11] W. Zhao and T. H. Go, "Quadcopter formation flight control combining MPC and robust feedback linearization," *Journal of the Franklin Institute*, vol. 351, no. 3, pp. 1335–1355, Mar. 2014, https://doi.org/10.1016/j.jfranklin.2013.10.021.

[12] Q. Quan, *Introduction to Multicopter Design and Control*. New York, NY, USA: Springer, 2017.

[13] F. Li, W.-P. Song, B.-F. Song, and H. Zhang, "Dynamic modeling, simulation, and parameter study of electric quadrotor system of Quad-Plane UAV in wind disturbance environment," *International Journal of Micro Air Vehicles*, vol. 13, Jan. 2021, Art. no. 17568293211022211, https://doi.org/10.1177/17568293211022211.

[14] Z. Cai, J. Lou, J. Zhao, K. Wu, N. Liu, and Y. X. Wang, "Quadrotor trajectory tracking and obstacle avoidance by chaotic grey wolf optimization-based active disturbance rejection control," *Mechanical Systems and Signal Processing*, vol. 128, pp. 636–654, Aug. 2019, https://doi.org/10.1016/j.ymssp.2019.03.035.

[15] Y. Liu *et al.*, "Robust nonlinear control approach to nontrivial maneuvers and obstacle avoidance for quadrotor UAV under disturbances," *Robotics and Autonomous Systems*, vol. 98, pp. 317–332, Dec. 2017, https://doi.org/10.1016/j.robot.2017.08.011.

[16] S. Abdelhay and A. Zakriti, "Modeling of a Quadcopter Trajectory Tracking System Using PID Controller," *Procedia Manufacturing*, vol. 32, pp. 564–571, Jan. 2019, https://doi.org/10.1016/j.promfg.2019. 02.253.

[17] A. Rezoug, M. Hamerlain, Z. Achour, and M. Tadjine, "Applied of an adaptive Higher order sliding mode controller to quadrotor trajectory tracking," in *International Conference on Control System, Computing and Engineering*, Penang, Malaysia, Nov. 2015, pp. 353–358, https://doi.org/10.1109/ICCSCE.2015.7482211.

[18] H. Loubar, R. Z. Boushaki, A. Aouati, and M. Bouanzoul, "Sliding Mode Controller for Linear and Nonlinear Trajectory Tracking of a Quadrotor," *International Review of Automatic Control*, vol. 13, no. 3, pp. 128–138, May 2020, https://doi.org/10.15866/ireaco.v13i3.18522.

[19] A. Eltayeb, M. F. Rahmat, M. A. M. Basri, and A. M. M. Mansour, "Adaptive Sliding Mode Control Design for the Attitude of the Quadrotor Unmanned Aerial Vehicle (UAV)," *IOP Conference Series: Materials Science and Engineering*, vol. 884, no. 1, Apr. 2020, Art. no. 012081, https://doi.org/10.1088/1757-899X/884/1/012081.

[20] J. Liu, *Sliding Mode Control Using MATLAB*. Cambridge, MA, USA: Academic Press, 2017.